J. Astrophys. Astr. (2022)43:17
https://doi.org/10.1007/s12036-022-09799-7

OBSERVATIONAL FACILITIES

Development of a new type of metallic mirrors for 21m MACE γ-ray telescope

V. K. DHAR[1], K. K. SINGH[1,*], K. VENUGOPAL[1], K. K. YADAV[1,2], R. KOUL[1] and R. BALASUBRAMANIAM[3]

[1]Astrophysical Sciences Division, Bhabha Atomic Research Centre, Mumbai 400085, India.
[2]Homi Bhabha National Institute, Anushaktinagar, Mumbai 400094, India.
[3]Control System Development Division, Bhabha Atomic Research Centre, Mumbai 400085, India.
*Corresponding author. E-mail: kksastro@barc.gov.in

MS received 22 October 2021; accepted 30 November 2021

Abstract. Major atmospheric Cherenkov experiment (MACE) is a ground-based imaging atmospheric Cherenkov telescope installed at Hanle ($\sim$4.3 km above sea level), Ladakh in the northern region of India. With a large parabolic reflector of 21 m diameter and 25 m focal length, MACE telescope is expected to explore the γ-ray Universe above 20 GeV. The tesselated light collector of MACE telescope employs 356 mirror panels each of size $\sim$1m $\times$ 1m. The individual panel comprises of 4 metallic mirror facets each of size $\sim$0.5m $\times$ 0.5m with a similar focal length. All 1424 mirror facets (356 $\times$ 4) are aligned in such a way that the whole reflector functions approximately as a single quasi-parabolic mirror of area $\sim$339 m^2 with a focal length varying from 25 m in the central region to 26.16 m on the periphery. Here, we describe the methodology for developing the metallic mirrors using the diamond turning technique. We also present the results from the testing and characterization of $\sim$1500 mirror facets, which qualify all the optical requirements of the MACE reflector. The testing of mirrors includes dimensionality, water ingress and environmental tests. The optical characterization of individual mirror facets is based on the measurements of focal length, spot size and reflectance.

Keywords. High energy astrophysics—gamma ray astronomy—imaging atmospheric Cherenkov telescopes—MACE—metallic mirrors.

1. Introduction

Ground-based γ-ray telescopes play a leading role to explore the non-thermal Universe in the GeV–TeV energy range using imaging atmospheric Cherenkov technique (Ong 1998; Aharonian *et al*. 2008; Hillas 2013; Funk 2015; Holder 2015; Di Sciascio 2019). This technique facilitates indirect detection of high energy γ-ray sources by measuring the Cherenkov light from the extensive air showers initiated by the γ-ray photons in the Earth atmosphere. It was discovered in 1934 that a charged particle moving faster than the speed of light in a transparent medium emits Cherenkov radiation (Cherenkov 1934) and the theory of this radiation is very well understood. As a high energy γ-ray photon enters the Earth's atmosphere, its energy is dissipated in the production of an electron-positron pair. The electron and positron further lose their energy by the bremsstrahlung process in the electric field of the atomic nuclei of constituent gases of the atmosphere. The process of e^-e^+ pair production and bremsstrahlung continues until the average energy per particle approaches the ionization energy. A swarm of relativistic charged particles produced in this way emit Cherenkov light while passing through the atmosphere. The Cherenkov emission angle depends strongly on the particle energy and atmospheric density and the Cherenkov photons emitted by the secondary charged particles (moving faster than the phase velocity of light in the air) reach the ground as a flash of light for a duration of $\sim$10 ns within a forward cone with an opening angle of $\sim$1° at high

This article is part of the Special Issue on "Astrophysical Jets and Observational Facilities: A National Perspective".

Published online: 19 March 2022

altitudes. This implies that the direction of emitted light nearly coincides with the primary particle direction. An extensive air shower from a small zenith angle initiated by an energetic cosmic γ-ray uniformly illuminates a circular light pool on the ground with a diameter of $\sim$250 m centered on the shower core. Therefore, an effective collection area of $\sim 5 \times 10^4$ m^2 is available on the ground to detect an extensive air shower produced by primary cosmic γ-rays. The Cherenkov radiation emitted by a cosmic air shower was first detected as a fast flash of light from the ground in 1953 (Galbraith & Jelley 1953). The Cherenkov photons can be focused to form an image of the air shower using an appropriate arrangement of mirrors in the ground-based instruments. The ground-based γ-ray telescopes employ full Earth atmosphere as a calorimeter and collect the Cherenkov photons from the entire development of the air shower initiated by a cosmic γ-ray and form the shower image at the focal plane. Hence, they are referred to as the imaging atmospheric Cherenkov telescope (IACT). Detection of high energy γ-rays from astrophysical sources using IACTs was started in the early 1990s by several groups worldwide (Hoffman *et al*. 1999; Catanese & Weekes 1999; Lorenz & Wagner 2012; Hillas 2013; Mirzoyan 2014; Singh & Yadav 2021). Subsequently, the advent of several state-of-the-art IACTs like Whipple (Weekes *et al*.1989), HEGRA (Mirzoyan *et al*.1994; Mirzoyan 1992), H.E.S.S. (Hinton *et al*.2004), VERITAS (Holder *et al*.2006), MAGIC (Cortina 2005), CANGAROO (Kubo *et al*.2004) and TACTIC (Koul *et al*.2007) has immensely benefited the researchers to explore the γ-ray Universe through ground-based observations. However, the faintness and optical characteristics of the Cherenkov light flash pose the biggest challenge in the cosmic γ-ray observations using IACTs. Large light collectors are needed to detect the faint Cherenkov light flashes with higher photon statistics in clear and dark nights. The relationship between a total number of Cherenkov photons produced from an air shower and energy of γ-rays initiating the shower is used to determine the threshold energy of an IACT. The threshold energy is defined as the minimum energy of γ-ray photons for which the signal-to-noise ratio is sufficient to adequately trigger the telescope (Aharonian & Akerlof 1997). The signal-to-noise ratio for an IACT is proportional to the square root of its light collector/reflector area and the threshold energy is inversely proportional to the signal-to-noise ratio (Fegan 1997; Mirzoyan 1997). Therefore, the threshold energy of an IACT can be lowered either by reducing the noise contribution from the light of the night sky or by maximizing the area of the light collector. Low threshold energy for an IACT is desired to achieve a good overlap with the energy band explored by space-based γ-ray detectors. Therefore, IACTs with a few 100 m^2 reflector area equipped with an array of multiple mirrors have proven to be excellent cosmic γ-ray detectors in the GeV–TeV energy range.

A new astronomical discipline primarily based on observations using IACTs is referred to as very high energy (VHE) or TeV γ-ray astronomy. This field of γ-ray astronomy has made very significant progress over the last three decades with the discovery of a large number of Galactic and extragalactic sources emitting GeV–TeV γ-ray photons. The astrophysical γ-ray emission from these sources is generally described by a falling power-law spectrum, resulting in very low photon statistics at the high energy end. Therefore, detectors with a large collection area are required to explore the γ-ray sky at high energies. The IACTs having big reflectors/light-collectors and photo-multiplier tube (PMT) based cameras at the focal plane are very efficient instruments with excellent angular resolution and strong background rejection power for the detection of GeV–TeV γ-ray sources in the Universe. In order to effectively explore the energy region beyond 10 GeV through ground-based observations, a large area major atmospheric Cherenkov experiment (MACE) has been recently set up by a group of Indian γ-ray researchers. The MACE telescope belongs to the category of state-of-the-art IACTs like MAGIC-I (Bradbury *et al*. 1995; Mirzoyan 1997) on the world map. In this paper, we present the details of mirror development for the reflector of 21 m diameter MACE γ-ray telescope. The paper is organized as follows. In Section 2, salient features of the MACE telescope are briefly described. The development of metallic mirror facets for the MACE light collector using the diamond turning technique is discussed in Section 3. The characterization of mirrors is presented in Section 4. Finally, we summarize the study in Section 5.

2. The MACE telescope

The MACE telescope is located 4.3 km above sea level at Hanle (32.8°N, 78.9°E), Ladakh in the northern region of India (Koul 2017). This high-altitude Himalayan desert region is among very few astronomical sites in the world with excellent atmospheric conditions for ground-based astrophysical

γ-ray observations. This site offers a very good year-round sky coverage with about 260 uniformly distributed dark and clear nights leading to an excellent duty cycle. A photograph of the MACE telescope structure and its installation at the site is depicted in Figure 1. The MACE telescope has three major subsystems: mechanical structure including drive system, an optical system including a quasi-parabolic light reflector and a PMT-based multi-pixel camera. The drive system of MACE telescope employs an altitude-azimuth mount on a 27 m diameter circular track and can provide a tracking accuracy of better than 1 arc-min in a wind speed of up to 30 km h^{-1}. A track and wheel design is followed for the azimuthal motion of the telescope. The entire weight of the telescope ($\sim$180 ton) is supported on uniformly spaced 6 wheels of 60 cm diameter each. Two azimuth drive wheels are coupled to three-phase, permanent magnet brushless AC servo motors through multi-stage gear-boxes for providing the azimuth motion. The elevation movement is provided through a gearbox coupled to the 13-section bull-gear assembly of an 11.6m radius. All the drives are provided with the counter-torque capability to avoid gear backlash error. The motors are driven by a pulse width modulated drive amplifiers powered by 480 V DC from a solar power station. The positions of the two axes are monitored by 25-bit absolute optical encoders with 20 arc-sec accuracy. Both the azimuth and elevation gear boxes also have high-speed options to move the telescope at a speed of 3° s^{-1} to quickly point the telescope in the direction of astrophysical transient events. The optical system of the MACE telescope involves a 21 m diameter mirror basket suspended from the 23m diameter stiffening ring, which is supported by two elevation brackets. These brackets are supported by diametrically opposite A-frame structures of height 15m each. The mirror basket is a two-layer structure having a rod and knot design with a square pitch of 1008 mm on the front end for the installation of mirror assemblies. Four planer booms supported by the stiffening ring hold a 1.5-ton camera assembly at a distance of 25 m from the mirror surface. The imaging camera at the focal plane of the telescope employs 1088 PMTs (6 stages, ETE, UK-make 9117 WSB) of 38 mm diameter each to detect the fast Cherenkov light flash of a few nanoseconds duration. The PMTs, arranged at a triangular pitch of 55mm, are provided with hexagonal front-coated compound parabolic concentrators for reducing the dead space between adjacent pixels and therefore enhancing their light collection efficiency. The angular size of light concentrators is 0.125° at the entry aperture and the whole camera covers a field of view of $\sim$4.36° $\times$ 4.03°. The camera is modular in design with 68 integrated modules of 16 pixels/channels each. The individual channel has its in-house signal processing electronics inside the camera.

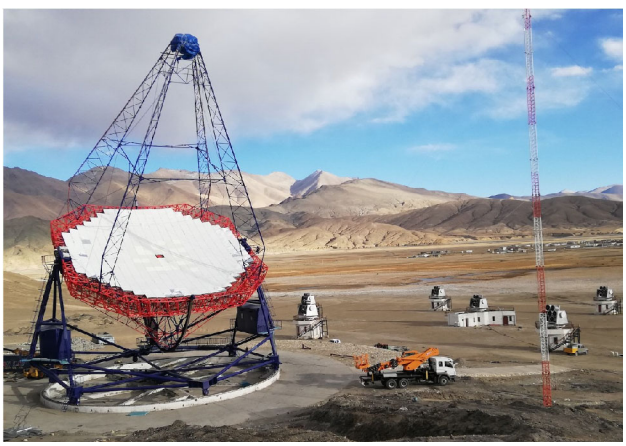

Figure 1. Structure and installation of the MACE telescope at Hanle site (4.3 km above sea level).

Detailed simulation studies carried out using CORSIKA (COsmic Ray SImulations for KAscade) software package suggest that the MACE telescope is expected to have a γ-ray trigger threshold energy of $\sim$20 GeV at low zenith angles below 30° (Borwankar *et al*. 2016). At high zenith angles of 40° and 60°, the trigger threshold energy increases to $\sim$40 GeV and $\sim$173 GeV, respectively (Borwankar *et al*. 2016). The total trigger rate of the MACE telescope for the 4 closed clusters nearest neighbor (CCNN) trigger with a single-channel threshold of 9.0 photoelectrons is $\sim$1 kHz with a maximum contribution of $\sim$840 Hz from protons in the low zenith angle range below 30° (Borwankar *et al*. 2020). The dynamic energy range of the MACE telescope is expected to be 20 GeV–10 TeV with a total trigger rate of $\sim$1 kHz in the low zenith angle range. Monte Carlo simulations show that the integral sensitivity of the MACE telescope for a point source with the Crab Nebula like spectrum above 31 GeV is 2.4% at 5σ statistical significance level in 50 h of observation (Sharma *et al*. 2017; Borwankar *et al*. 2020). Also, they show that the MACE telescope has lower threshold energy than the MAGIC-I telescope and its integral flux sensitivity is better than that of the MAGIC-I telescope for γ-ray energies below 150 GeV (Borwankar *et al*. 2020). The angular resolution of the MACE telescope is estimated as $\sim$0.21° in the energy range of 30–50 GeV and this improves to $\sim$0.06° in the energy band 1.8–3 TeV (Borwankar *et al*. 2020). The telescope is expected

to have energy resolutions of $\sim$40% and $\sim$19% in the energy bands 30–50 GeV and 1.8–3 TeV, respectively.

3. Mirror development for MACE telescope

The specifications of the light collector/reflector for IACTs like MACE are less stringent than the conventional optical telescopes in many aspects. First, the IACTs are equipped with large light collectors with tesselated structure (array of multiple tens or hundreds of mirrors) whereas optical telescopes generally employ a single mirror. Second, the point spread function (PSF) of an IACT ($\sim$few arcminutes) can be larger than that of the optical telescopes. Normally, the PSF of the Cherenkov telescope is a factor of 2 smaller than the camera pixel size for an on-axis beam of light. The focal length of IACTs is usually selected to keep the focal length to aperture diameter ratio (f/d) between 1.1 and 1.3 where the optical aberrations are small enough to make a good quality shower image at the focal plane. With a good quality imaging of the shower, the IACTs can reconstruct the direction and energy of the primary γ-ray photons and distinguish them from the huge cosmic ray background. Also, the mirrors used in the reflectors of the IACTs should be robust, light weight and high reflectance in the wavelength range 280–600 nm well-overlapping with the Cherenkov spectrum peaking at blue.

3.1 *MACE light collector*

The light collector of MACE telescope features a 21 m diameter quasi-parabolic dish with $f/d = 1.2$ type optical system. The quasi-parabolic design of such a large reflector helps in greatly reducing the optical aberration of the telescope as well as maintaining the temporal profile of Cherenkov flash. This provides a total light collector area of $\sim$339 m^2 and an effective focal length of $\sim$25 m. To achieve such a large light collector area, the reflector of MACE telescope is segmented into 1424 small spherical mirror facets of size 0.488m $\times$ 0.488m each with varying focal lengths between 25.0 m and 26.25 m. Four such mirror facets with similar focal length are mounted on a single panel of size 0.948m $\times$ 0.948m each and are manually aligned in such a way that the resulting panel behaves like a single spherical reflecting surface. The panel position in the telescope basket is optimized for the best parabolic approximation. Therefore, the MACE light collector has 356 mirror panels mounted on the telescope basket with focal lengths gradually increasing from the center of the basket towards the periphery. The graded focal length of mirror facets helps in minimizing the on-axis spot size and temporal spread in a spot at the focal plane. The mirrors used in the MACE reflector have metallic facets made up of aluminum alloy supported by the honeycomb structure. The advantage of honeycomb structure is that in addition to significantly reducing the telescope weight, it also helps in providing stiffness.

3.2 *Need for metallic mirrors*

Light collectors in the IACTs need mirrors with high reflectivity in the ultraviolet and optical wavelength band (280–600 nm). Glass mirrors with a front surface coating of aluminum (Al) have generally been preferred in the early IACTs. However, diamond milled aluminum mirrors were first time (in 2003) used in the 17 m diameter reflector of the MAGIC-I telescope (Doro *et al*. 2008). Due to their large aperture diameter, the reflectors in big IACTs like MACE cannot be protected by a dome and therefore the mirrors will be constantly exposed to the environment of varying seasons (Mirzoyan *et al*. 1996). This may lead to a significant loss of reflectivity over a period of a few years and re-coating of mirrors is frequently required for continuous operation of IACTs with high duty cycle. Maintenance of glass mirrors is also very difficult in the open field instruments. The night temperature of sites for IACTs during winter becomes very low (-30°C at Hanle). Therefore, the materials used in the mirrors must retain a good impact strength at low temperatures. Apart from these natural limitations, the development of large spherical glass mirrors as per the specifications of IACTs poses a technological challenge and the overall weight of the telescope also increases significantly by the use of glass mirrors. Thus, the choice of mirror facets in the reflector of a large IACT is driven by cost, weight, durability and installation on the basket. Metallic mirrors are found to be the best candidates to overcome most of the challenges mentioned above, compared to glass mirrors which suffer from several drawbacks like being fragile and faster degradation of the surface reflectance.

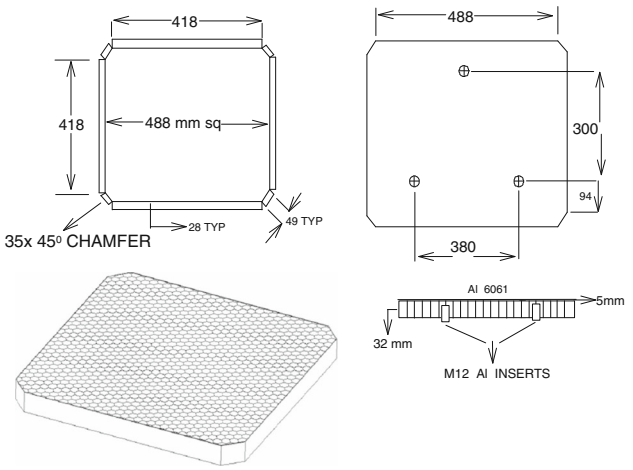

Figure 2. Step involved in the preparation of raw blanks for MACE mirrors.

3.3 *Metallic mirror fabrication by diamond turning technology*

Gold, Silver and aluminum are the metals which exhibit the highest reflectance of light in different wavelength bands. Gold and Silver reflect mostly infrared and visible lights, respectively. Whereas, aluminum together with its longer durability is a good choice for reflecting ultraviolet and visible light. The aluminum alloys with moderate impurities are found to fulfill the requirements of a reflector to be employed in the IACTs. Steps involved in the production of mirror facets using aluminum 6061 (Al 6061) for the reflector of MACE telescope are described below:

- *Preparation of raw blanks:* The alloy Al 6061 exhibits a very strong corrosion resistance with high reflectivity as compared to other alloys. Step by step preparation of the raw blanks for MACE mirror facets is depicted in Figure 2. More than 1500 raw blanks have been prepared by HEXCEL[1] and supplied to our industrial partner Mechvac Fabricators (India) Private Limited. The front face of each mirror is made up of Al 6061 plate (AlMgSi0.5 or AlMgSi1.0) with a thickness of $\sim$5 mm and the back of the mirror facet is $\sim$1 mm thick Al (5251H122) plate. A structurally rigid mirror blank is prepared by sandwiching a 26 mm thick HEXCEL HexWeb Al honeycomb structure[2] between the front plate and back sheet using suitable structural adhesives (REDUX 610 resin) followed by curing. REDUX 610 resin is a modified flame retarded epoxy film adhesive with curing at 250°F and is known to be UV-resistant.[3] The outer rim of the HEXCEL plate is filled with UV resistant foam to avoid degradation. The density of honeycomb substrate is $\sim$60 kg m^{-3}. The honeycomb structure is manufactured by bonding together sheets of 3000 series Al alloy foil and is expanded to form a cellular honeycomb configuration with a cell size of 6 mm. An organic coating of CR III (chromate-based organo-metallic polymer) using physical vapor deposition (PVD) technology is applied to the foils to protect the corrosive atmosphere. Al HEXCEL honeycomb structure offers a better heat conductivity and also ensures rigidity without increasing the weight of the mirror facets. It has a compressive yield strength of 4.34 MPa, compressive modulus of 1.02 GPa and a shear modulus of 0.26 GPa with a shear strength of 1.48 MPa. Each of these honeycombed mirror facets are supported on three points for holding the mirror facets.
The mirror facets are fabricated from the 0.488m $\times$ 0.488m square blanks with the corners cut and folded to form a chamfer of 35 mm. The sides and corners are very carefully folded to form a box and resin is used to seal all joints to avoid any leakages. Considering all the dimensions into consideration the total thickness of each facet turns out to be $\sim$32 mm with a weight of 4–5 kg. An ultrasonic test is performed for honeycomb bonding in the blank by using a pulser as a transducer to generate high-frequency ultrasonic energy. The sound energy propagates through the materials in the form of waves. If there is any discontinuity (such as a crack) in the path, part of the energy is reflected back from the flawed surface, thereby detecting the cracks. After the honeycomb bonding is found to be satisfactory, three Al inserts are also put with the help of redux for clamping the mirror on the panel. A 3-arm ball and socket arrangement with male and female contraptions has been made to hold the mirror facets and 0.948 m $\times$ 0.948 m panel together with the help of studs. The purpose of this arrangement is to enable the alignment of four mirror facets on the back end panel in such a way that they have a single focus. Mirror back paints are used for

[1] https://www.hexcel.com.

[2] https://www.hexcel.com/Resources/DataSheets/Honeycomb.

[3] https://www.hexcel.com/Resources/DataSheets/AdhesivesDataSheets.

protecting the backside of facets from overheating due to intense sunlight at the Hanle site. As such direct sunlight does not fall on the mirror facets since the MACE telescope is parked with the backside of the reflector facing North direction during day time.

- *Dimensionality and water ingress:* The dimensions and the chamfer size of each raw blank are carefully measured to exactly match with the requirements of the mirror basket of the MACE telescope. A water ingress test is also carried out on individual raw blanks in order to avoid any minor crack (invisible to the naked eye) in the mirror facet. This helps in reducing the possibility of degradation due to humidity entering through the small crack inside the mirror facet. This is done by weighing the raw blank and then keeping it immersed into hot water at a temperature of $\sim$80°C for about 30 min. If there is any crack present in the blank, air bubbles emanate while the mirror is kept immersed in the hot water. Also, the blanks are immediately weighed again after they are taken out of the water. An increase in the weight implies that there is some water retention through the cracks in the blank. REDUX 610 resin is used to avoid any leakages.
- *Computer numerical control machining:* The raw mirror blanks having honeycomb structured support of 0.488m $\times$ 0.488m are initially machined on a large size computer numerical control (CNC) lathe before generating the finished mirror surface. CNC machining is employed to remove layers of material from the blank to get an approximate spherical shape with the required radius of curvature (twice the focal length of the mirror facet). The material removal process is followed by a finish machining which is maintained by a tool with a large nose radius with multiple machining passes. The machining parameters like cutting speed (200–240 rpm), depth of cut (100–120 μm), feed rate (80–100 mm min^{-1}), and tool parameters such as material, nose radius, rake and clearance angles, clamping method, and clamping forces are critically optimized to minimize residual stresses and distortion due to the delicate nature and anisotropy of the honeycomb support and keeping in mind to improve the productivity. The machined spherical surfaces are measured by a coordinate measuring machine (CMM) with a pre-defined measuring cycle to avoid measurement errors. Once the blanks are machined and measured, they are kept in atmospheric condition for a few days to relieve the residual stress developed during machining processes.
- *Diamond turn machining:* Traditional finishing process, mainly abrasive based, generate random surfaces with superior finish, but lack control on maintaining the size and shape of the surface being polished. They are more suitable for flat-type surfaces. For generating spherical mirror surfaces of varying focal length (like the present case), traditional finishing processes cannot economically be employed. Diamond turn machining (DTM), which is also referred to as deterministic nano regime machining process, is capable of controlling the size, shape and surface finish in a faster and economically viable way (Sugano *et al.* 1987). The surface finish achieved by the DTM process is limited to about 10 nm, which is acceptable for IACT applications (Basteiri *et al.* 2003). However, during the actual DTM process, the diamond tool may create humps of irregular shape due to the deposition of removed material on both sides of its path. These humps scatter off the impinging light and affect the reflectance of the mirror surface. This along with other losses due to scratches and deposition of dust leads to a reduction of 10–15% in the actual reflectance of the mirror (Mirzoyan *et al.* 2019). In the development of metallic mirror facets for the MACE telescope, Precitech-make, model-nanoform 700 ultra DTM has been employed for finishing machining. The machine, shown in Figure 3, has a typical spindle run-out of 50 nm and positional accuracy of a few tens of nm. It is built with an aerostatic spindle and hydrostatic table. Since undue clamping forces are likely to distort the component after the release of the clamping, a special mirror blank holding fixture has been designed to minimize the effect of clamping forces on the mirror blank surface. The effect of footprint error is also minimized in this fixture. The DTM is provided with two tool stations, one for prefinishing and another for the final finishing of the mirror surface. A single-crystal diamond tool with a typical nose radius of 5 mm, sharpness of 200 nm and a feed rate of 5 μm per revolution with direction-controlled mist coolant is used for machining. Generally, three machining-cum-finishing passes have been used

Figure 3. A finished mirror facet for the MACE telescope on DTM.

to achieve size and shape control. Spindle rotational speed is optimized to achieve the desired surface finish. The direction of the application of the mist coolant is vital to control the chip flow, which should not get entangled as well as scratch the finished surface. Typically, the distance, tool travels on the surface for machining is approximately 75 km per machining pass. Single crystal diamond being the highest wear-resisting material that lasts for a longer machining time. Figure 3 shows the final finished mirror on the DTM. The quasi-parabolic reflector of the MACE telescope employs a total of 1424 mirror facets with focal lengths ranging from 25 m to 26.16 m and is divided into 11 zones with different focal lengths. The accuracy of the mirror facet focal length for each zone is ±50 mm.

- *Surface protection coating:* Protection of reflecting surface of the DTM finished mirror facet is very important for longer durability since mirrors employed in the telescope reflector are continuously exposed to the open environment. A thin film coating of any refractive index to the metallic surfaces results in the reduction of reflectivity at all wavelengths except one. For Al mirrors, coating of silicon dioxide (SiO_2) preserves the reflectivity at a wavelength $\lambda \sim 550$ nm. However, if a thin-film is thinner than the wavelength, the change in reflectance is negligible. Typically, the thickness of thin film coating to protect the mirror surface is chosen as a multiple of $\lambda/4$ for minimum reduction of the reflectance in the wavelength range of 300–700 nm (Mirzoyan *et al*. 2019). For the MACE mirror facets, the purpose of SiO_2 coating is to provide a hard and scratch-resistant layer with a little compromise on the reflectivity and is not intended for any enhancement in the reflectance. A batch vacuum coating machine (Balzers 1250) has been used for SiO_2 coating to the MACE mirror facets. Two mirror facets are simultaneously loaded in the vacuum chamber and SiO_2 is filled in a crucible. The machine creates a vacuum of 2.5×10^{-5} mbar and SiO_2 in the crucible is heated by the electron beam. The vapor formed due to SiO_2 melting is gradually deposited to the Al facets. The machine parameters are programmed to deposit a layer of SiO_2 with a thickness of $\sim$120 nm in a total coating time of $\sim$8 h. An in-built quartz crystal monitor in the coating system is used to measure the coating thickness. The uniformity in the coating is ensured by measuring the thickness at predefined places. The coating adhesion is tested by the standard tape tests. The adhesion strength of SiO_2 is measured by applying a 3M white tape with an adhesion strength of 15N per 25 mm to the coated surface of the mirror facets. No damage to the surface is observed during this snap test. This suggests that the SiO_2 coating adhesion is better than 15N per 25 mm for the mirror facets used in the MACE reflector.

4. Characterization of mirror facets

The basic optical requirements for individual diamond-turned mirror facets are focal length, spot size, and reflectance as desired by the MACE light collector. The focal length of a given IACT is decided by the expected field of view of the single telescope which is governed by the maximum impact parameter detectable by the IACT. The optical point spread function (PSF) is chosen to provide an efficient γ-hadron separation and to match the used pixel size (angular size of the PMT) in the focal plane of the telescope. Individual mirror facets are required to focus light from a point source onto a single pixel at the camera plane. Therefore, all the diamond turning machined mirrors have been subsequently tested for the focal length and spot size at the focal point for their qualification predefined by the specification of

the MACE telescope. In addition to these parameters, each mirror facet is expected to have a very high reflectance (above 80%) in order to effectively detect the dim Cherenkov light from an extensive air shower. Details of the testing procedure and measurements of more than 1500 mirror facets for the MACE telescope are described below.

4.1 *Experimental setup*

A $2f$ (f being the focal length of the mirror facet) test facility has been setup to characterize the metallic mirror facets for the MACE light collectors. A point-like light source is placed at a distance twice the mirror focal length ($2f$) on its optical axis to uniformly illuminate the reflecting surface. The geometrical optics suggests that the reflected light will form an image at $2f$ distance and actual spot size at focal plane will be half of that at $2f$ for parallel rays of incident light. We have employed a green diode laser ($\lambda \sim 532$ nm) with a beam diameter of ~ 2 mm, a typical beam divergence of ~ 1.3 mrad, and a power rating of ~ 3 mW as a light source. The laser is placed at a distance of 50 m from the mirror facet. The mirror facets are fixed on a holding assembly directly facing the laser beam. A short focal length convex lens (~ 5 cm) is employed in front of the laser as a beam expander. This expands the highly directional laser beam so that an area of about 1m $\times$ 1m can be uniformly illuminated at a distance of 50 m. The mirror facets are placed at the center of this uniformly illuminated spherical area. A movable white screen at the focal plane is used to get the position of a minimum size of the spot formed by the reflected light from the mirror facet. This experimental setup is shown in Figure 4. A distance meter (Leica Disto-D5) with a digital color point finder display and a 45° tilt sensor, is used to measure the distances with an accuracy of 1.5 mm.

4.2 *Spot size and focal length measurements*

Individual mirror facet after diamond turning and SiO_2 coating is fixed at mirror holder assembly and uniformly illuminated by the laser light. The distance between mirror facet and laser is fixed at $u = 50$ m. The reflected light is brought to a sharp focus on a white screen which can move back and forth. The screen position is adjusted to obtain the smallest possible spot formed by the reflected light. The distance between this position of screen and mirror facet is measured as v. Using the measured values of u and

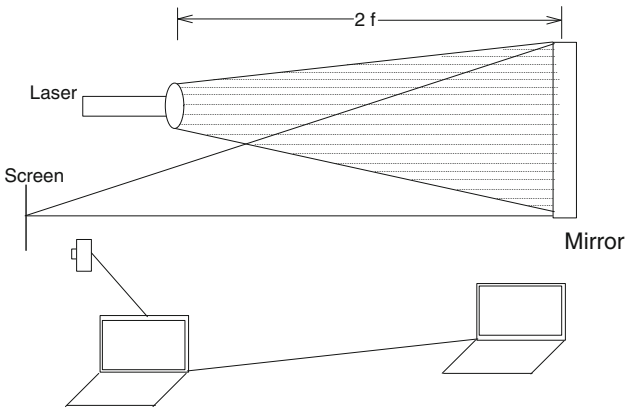

Figure 4. Experimental setup based on $2f$ method for optical measurements of the metallic mirror facets for the MACE telescope.

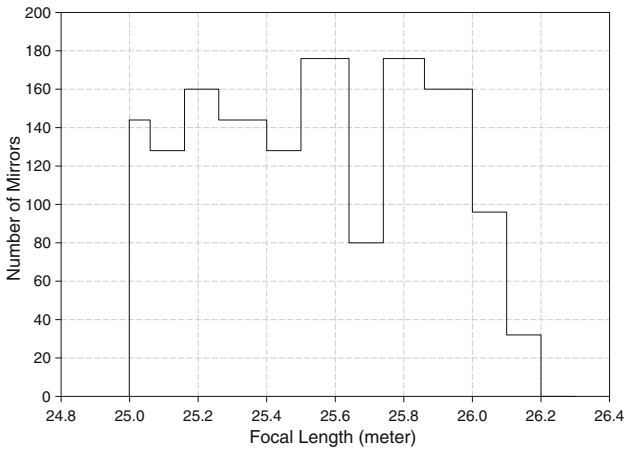

Figure 5. Frequency distribution of the measured focal lengths of the spherical mirrors for the MACE light collector.

v, the focal length (f) of a given mirror facet is obtained from the mirror formula:

$$\frac{1}{f} = \frac{1}{u} + \frac{1}{v}. \quad (1)$$

The focal lengths of more than 1500 diamond-turned metallic facets have been estimated using Equation (1). The distribution of measured focal lengths for the mirror facets which qualify the criterion of the MACE light collector is shown in Figure 5. The focal length values vary between 25 m and 26.2 m as decided by the paraboloid design of the 21 m diameter light reflector employed in the MACE telescope.

After obtaining the position of the smallest possible spread of the reflected light, we manually measure the D_{80} (defined as the diameter of a circle centered at the spot gravity, containing about 80% of the reflected light) of the spot by using pre-drawn circles of

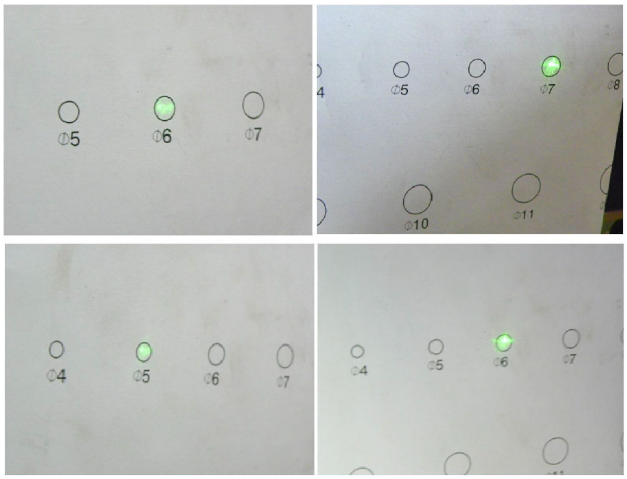

Figure 6. Manual measurement of the spot size of four different mirrors. The green spots are the minimum possible spread of the reflected light at the focal plane.

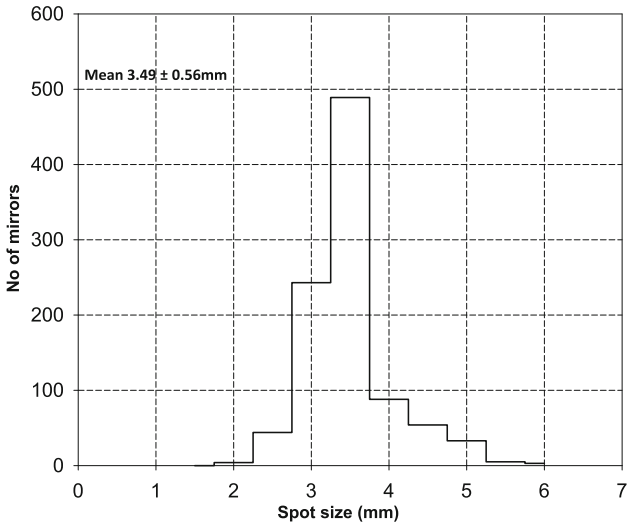

Figure 7. Frequency distribution of measured spot size of the mirror facets selected for MACE telescope.

diameter between 4 mm and 15 mm on the screen. A representative picture of this measurement is depicted in Figure 6 for four mirror facets. The mirror facets with $D_{80} \leq 6$ mm are accepted for the MACE reflector, provided the corresponding focal length lies in range 25–26.2 m (Figure 5). The distribution of spot size measurements for the qualified mirrors is presented in Figure 7. We observe that the mean of spot size for more than 1500 diamond-turned metallic mirrors is ~ 3.5 mm, which is much less than the predefined value of $D_{80} \leq 6$ mm. The reflected light from a given mirror surface (exhibiting relevant surface roughness) consists of a specular reflection (following the law of reflection) and a scattered component (diffusely reflected). The total integrated scatter (TIS) from a given mirror surface depends on the root mean square surface roughness (σ) and the wavelength of light (λ). Under paraxial smooth surface approximation (for normal incident light), loss due to diffuse reflection is estimated as (Harvey *et al.* 2012; Mirzoyan *et al.* 2019)

$$\mathrm{TIS} = \left(\frac{4\pi\sigma}{\lambda}\right)^2. \tag{2}$$

A roughness tester (Mitutoyo SURFTEST SJ-410) is used to measure σ of the metallic mirror facets developed for the MACE telescope. For $\lambda = 400$ nm and $\sigma = 10$–15 nm (measured for a sample of facets), the corresponding scatter loss is obtained to be $\mathrm{TIS} \sim (9.8 - 23)\%$. Therefore, the absolute reflectance of the mirror facets is reduced (by an average value of $\sim 15\%$) due to their surface roughness. This will slightly modify the measured spot size.

Apart from the manual measurement, we have also performed image processing for calculating the D_{80} values. The image of each spot, captured using a 10 mega-pixel digital camera, is converted into a gray-scale image. This image is then digitized by converting the pixel intensity into digital counts. The pixel in the image with the brightest intensity (centroid) is identified and concentric circles are drawn around it with an increase in diameter of the new circle by one pixel. The total number of digitized counts in each circle are recorded. Background counts are also recorded from the image frame itself and these are subtracted from the pixel counts. A normalized intensity plot as a function of number of pixels (as shown in Figure 8) contained in each circle is obtained. Knowing the conversion scale from the actual measurement of the maximum extent of image (D_{100}), the value of D_{80} for a given mirror facet can be easily calculated. An excellent matching between manual measurements of D_{80} and that derived from the image processing is obtained. It is important to mention here that since we have individually tested more than 1500 mirror facets, it is quite time-consuming to process the image for all mirrors. Therefore, image processing has been done randomly to cross-check the manual measurements for a few samples.

4.3 *Surface accuracy and reflectivity measurements*

Interferometric measurements have been employed to check the precision of surface flatness of diamond-turned metallic facets. Surface accuracy is measured with a coordinate measuring machine. All the mirror

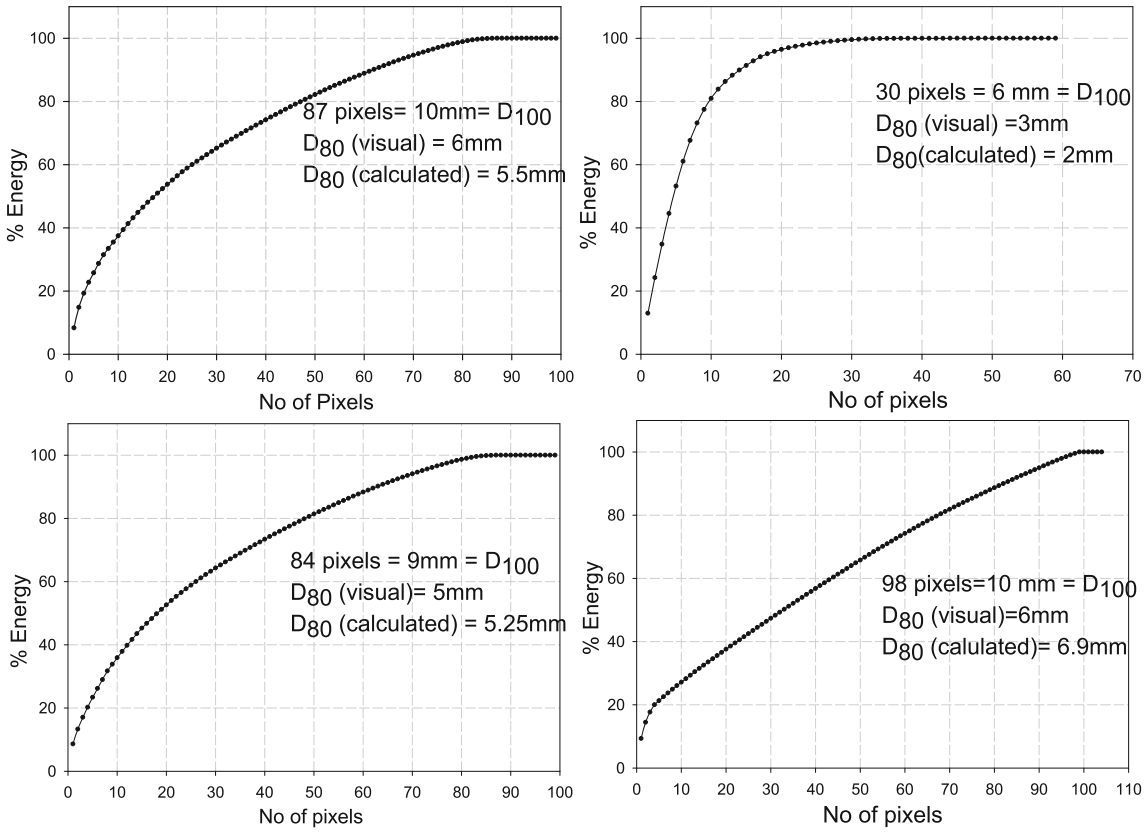

Figure 8. Image processing of the spot size for four mirror facets.

facets with an accuracy of a few μm and surface finish <20 nm have been selected for the MACE light collector. Another important requirement of these mirror facets is the global reflectance above 80% in the wavelength range $\lambda = 270$–700 nm. The reflectivity measurements have been carried out by UV-1800 Shimadzu double beam spectrophotometer. For this measurement, we have also fabricated baby mirrors referred to as *witness samples* of radius 24 mm. These witness samples associated with individual mirror facets go through the same manufacturing process as the mother mirror facets. Figure 9 shows the reflectivity measurements of four sample mirrors with the best and worst-case scenarios. It is evident from the figure that a mean reflectance of about 85% is achievable for the diamond-turned metallic mirrors developed for the MACE telescope. For the varying thickness of the SiO_2 coating, the peak of the reflectance curve will shift to different wavelengths. If the coating is thick, the peak reflectance shifts towards longer wavelengths and vice versa (Figure 9). It is important to note here that the non-optimal thickness of SiO_2 coating can reduce the reflectance in the wavelength band of interest, but it does not contribute significantly in the scattered component of the light.

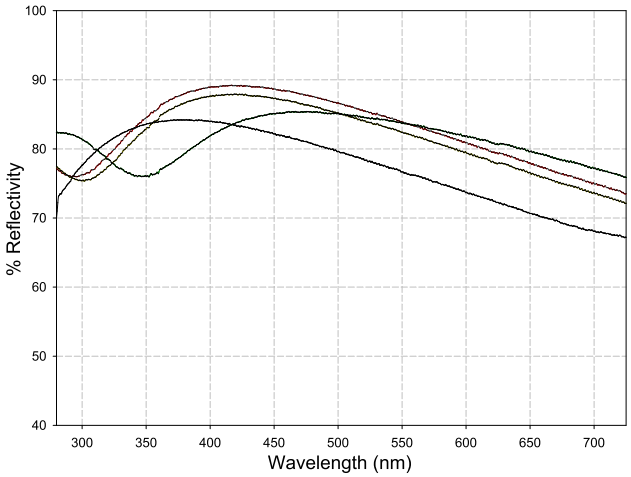

Figure 9. Spectral surface reflectivity measured for four mirror samples with highest and lowest reflectance.

The reflectance in the whole individual mirror surface varies within $\pm 2\%$.

4.4 *Environmental testing*

Apart from their optical properties, the mechanical stability of the metallic mirrors under extreme weather

conditions at astronomical sites like Hanle is a very important issue. We have performed a few environmental tests with physical conditions similar to the actual conditions at Hanle on a sample of mirror facets. This environmental test referred to as *Severity*, is conducted in two phases. In the first phase, the temperature of sample facets is decreased from the ambient temperature to −30°C in a time span of 1.5 h. The facets are left at −30°C for 2 h and then the temperature is again increased to +30°C in 1 h duration and left at +30°C for 2 h. The temperature is decreased to the ambient temperature in 0.5 h. This process of increase/decrease in temperature constituted one cycle. A total of 76 such cycles have been performed on the sample facets. In the second phase, the temperature was changed from +30° to −40°C in a period of 1 h and left at this temperature for 2 h. The temperature was again increased from −40° to 40°C in 1 h and this temperature is maintained for 2 h followed by cooling from 40° to 30°C in 1 h. This constitutes one cycle. Such 24 cycles are repeated. Thus, a total of 100 cycles have been performed on the sample facets in a period of 30 days. The spot size of these sample mirrors are checked before and after the environmental testing. The sample facets are observed to reproduce their earlier spot size, reassuring that metallic mirrors manufactured for the MACE telescope can withstand the harsh climatic conditions at Hanle. In order to check the long-term durability and mechanical stability in the conditions of outdoor usage, a few metallic mirror facets were exposed at the TACTIC observatory (Singh & Yadav 2021) for three years. A degradation of ∼7% was observed in the reflectance after three years of outdoor exposure. Whereas, no appreciable change in the spot size, as well as mechanical stability, was observed.

5. Summary

More than 1500 metallic mirror facets of size 0.488m × 0.488m each have been manufactured using the diamond turning technique for the 21 m diameter light collector of the MACE telescope. The MACE telescope has been recently installed at Hanle (∼4.3 km above sea level), India. A total of 1424 facets are employed in the telescope to get a collection area of ∼339 m^2. Honeycomb structure inside the mirror facets provides high rigidity and low weight as compared to glass mirrors. The Al 6061 alloy used for reflecting surfaces of the mirror facets are not affected by the cold working conditions at high altitudes like Hanle. Due to the large size of the MACE reflector, it is not practically possible to cover the telescope using any dome during the day and OFF time. Therefore, all the mirror facets have been coated with SiO_2 for protection against changing environmental conditions at the Hanle site. Some of the important advantages of using metallic mirror facets over glass mirror for the MACE telescope reflector are: weight is reduced drastically (∼25%), simpler handling with no risk of breaking, cost-effective production with varying focal lengths and less prone to defects in case of corrosive attacks. Major factors which enhance the Al mirror life are used in dry climate conditions compared to the humid climate, usage in low pollution areas and operation in non-salt environments. Due to all these favorable factors at the Hanle site, we expect that these mirrors will serve over at least a decade.

Acknowledgments

The authors are thankful to the anonymous reviewer for his/her suggestions in improving the manuscript. They also thank their colleagues from the Astrophysical Sciences Division, Center for Design & Manufacturing, and Atomic & Molecular Physics Division at Bhabha Atomic Research Centre for their contributions at different stages in the development of metallic mirror facets for the MACE telescope. Help rendered by Dr S. K. Ghosh from the Materials Processing & Corrosion Engineering Division for surface roughness measurements is duly acknowledged. The authors are also thankful to the Electronics Corporation of India Limited (ECIL) and Paras Defence & Space Technologies, Mumbai (earlier Mechvac India Limited) for providing the mirror facet development facilities. They dedicate this study to the memory of their colleague Dr A. K. Tickoo who passed away in February 2021.

References

Aharonian F. A., Akerlof C. W. 1997, Rev. Nucl. Part. Sci., 47, 273
Aharonian F. A. *et al.* 2008, Rep. Prog. Phys., 71, 096901
Bastieri D. *et al.* 2003, ICRC, 5, 2919
Borwankar C. *et al.* 2016, APh, 84, 97
Borwankar C. *et al.* 2020, NIMPA, 953, 163182
Bradbury S. *et al.* 1995, ICRC, 1, 1051
Catanese M., Weekes T. C. 1999, PASP, 111, 1193

Cherenkov P. A. 1934, Doklady Akademii Nauk SSSR, 2, 451
Cortina J. 2005, Ap&SS, 297, 245
Di Sciascio G. 2019, JPCS, 1263, 012003
Doro M. *et al.* 2008, NIMPA, 595, 200
Fegan D. J. 1997, JPhy. G, 23, 1013
Funk S. 2015, ARNPS, 65, 245
Galbraith W., Jelley J. V. 1953, Nature, 171, 349
Harvey J. E. *et al.* 2012, Opt. Eng., 51, 013402
Hillas A. M. 2013, APh, 43, 19
Hinton J. A. *et al.* 2004, NA Rev., 48, 331
Hoffman C. M. *et al.* 1999, Rev. Mod. Phys., 71, 897
Holder J. *et al.* 2006, APh, 25, 391
Holder J. 2015, arXiv: 1510.05675
Koul R. *et al.* 2007, NIMPA, 578, 548
Koul R. 2017, Curr. Sci., 113, 691
Kubo H. *et al.* 2004, NA Rev., 48, 323
Lorenz E., Wagner R. 2012, EPJH, 37, 459
Mirzoyan R. 1992, Towards a Major Atmospheric Cerenkov Detector for TeV Astro/particle Physics, 239
Mirzoyan R. *et al.* 1994, NIMPA, 351, 513
Mirzoyan R. *et al.* 1996, NIMPA, 373, 153
Mirzoyan R. 1997, Nucl. Phys. B Proc. Suppl., 54, 350
Mirzoyan R. 2014, APh, 53, 91
Mirzoyan R. *et al.* 2019, APh, 105, 1
Ong R. A. 1998, Phys. Rep., 305, 93
Sharma M. *et al.* 2017, NIMPA, 851, 125
Singh K. K., Yadav K. K. 2021, Universe, 7, 96
Sugano T. *et al.* 1987, CIRP Annals, 36, 17
Weekes T. C. *et al.* 1989, ApJ, 342, 379